Spin-spin interaction between polarized neutrons and polarized ^{27}Al, ^{59}Co, and ^{93}Nb from dispersive optical model and coupled-channel analyses

M. M. Nagadi,* G. J. Weisel,† and R. L. Walter
Department of Physics, Duke University, Durham, North Carolina 27708, USA and Triangle Universities Nuclear Laboratory, Durham, North Carolina 27708, USA

J. P. Delaroche and P. Romain
Commissariat à l'Energie Atomique, Service de Physique Nucléaire, DAM/DIF/DPTA Boîte Postale 12, 91680 Bruyères-le-Châtel, France

(Received 9 August 2004; published 10 December 2004)

Coupled-channel and dispersive-optical model analyses of published neutron scattering and reaction data for ^{27}Al, ^{59}Co, and ^{93}Nb at incident energies between 0.1 and 80 MeV have been performed. The resulting potentials are used to place constraints on the determination of the spin-spin interaction from published spin-spin cross-section measurements. For the three nuclei, the strength of the central real spin-spin potential, which was taken to have a surface plus volume shape, was found to be small. Volume integrals for this central potential component were determined to be in the 4–7 MeV fm^3 range and to decrease somewhat as mass number increases.

DOI: 10.1103/PhysRevC.70.064604 PACS number(s): 24.10.Ht, 25.40.Dn, 24.70.+s, 28.20.Cz

I. INTRODUCTION

More than 40 years ago, Feshbach suggested that the nucleon-nucleus interaction should include a spin-spin term V_{ss} that stems from the spin-spin component of the nucleon-nucleon interaction [1]. Since then, a number of experiments have been designed to measure the properties of the spin-spin potential. One type are depolarization measurements of polarized protons incident on unpolarized targets. A second type are transmission measurements of polarized neutrons passing through polarized targets.

The information on V_{ss} that has been extracted in both types of experiments includes uncertainties related to (i) the precision with which the measurements were performed, and (ii) insufficient knowledge of reaction mechanisms. For instance, as Ref. [2] shows, the analysis of depolarization measurements requires a proper treatment of quadrupole spin-flip for target nuclei with spin $I > 1/2$. Also, large spin-spin effects observed in transmission measurements at low incident energies may be accounted for by compound nucleus effects [3,4]. Despite these uncertainties attached to the phenomenological determination of V_{ss}, a consensus was formed: the spin-spin interaction is weak, with a strength of the order of 1 MeV. This empirical result has been confirmed in high-precision transmission measurements using polarized neutrons [5,6] and supported by theoretical predictions based on a microscopic folding model [7]. Relatively recent depolarization studies of proton elastic scattering include Refs. [8–10]. Even though the spin-spin interaction is small in magnitude, it is important to know its size. The aim of the present work is to infer the strength and radial shape of this potential component from phenomenological optical potential analyses of neutron transmission measurements available for the medium mass nuclei ^{27}Al, ^{59}Co, and ^{93}Nb.

Analyses of the spin-spin cross section, σ_{ss}, have mainly been performed using spherical optical models (SOM) that include either a central or a tensor spin-spin term [11], and that often employ global SOM parametrizations. Since the global SOM potentials of Refs. [12,13] were not intended for model predictions at incident energies below 10 MeV and were designed to describe the gross scattering and reaction properties of many nuclei, they may not be realistic enough to obtain a precise determination of spin-spin potentials. The new global SOM of Ref. [14] models data at energies from 1 keV to 200 MeV and yields improved fits over earlier global models. However, rather than using this model, we prefer to develop custom optical models that are not weighted by high-energy data. By focusing our optical model descriptions on the low energy regime, we hope to improve our determination of the spin-spin potential for the $\vec{n}+{}^{27}\vec{\mathrm{Al}}$, $\vec{n}+{}^{59}\vec{\mathrm{Co}}$, and $\vec{n}+{}^{93}\vec{\mathrm{Nb}}$ systems.

The present paper builds a dispersive optical model (DOM) dedicated to $\vec{n}+{}^{93}\vec{\mathrm{Nb}}$ up to 80 MeV in order to predict the spin-spin cross sections for this scattering system. We chose the DOM because it provides a more realistic description of low-energy elastic scattering than does a conventional SOM [15]. Use of an SOM or DOM can be questioned when the target nuclei are deformed. Since ^{93}Nb is a spherical nucleus in its ground state [16], there was no need to consider a deformed potential using the coupled-channels model (CCM). For $\vec{n}+{}^{27}\vec{\mathrm{Al}}$ and $\vec{n}+{}^{59}\vec{\mathrm{Co}}$, the present paper uses both the DOM potentials and the CCM analyses of Ref. [15] to investigate the spin-spin cross sections for these systems.

*Permanent address: Department of Physics, King Fahd University of Petroleum and Minerals, Dhahran, Saudi Arabia.

†Permanent address: Department of Physics, Penn State Altoona, Altoona, PA 16601.

TABLE I. DOM potential parameters. Energy and depths are in MeV. Geometries and lengths are in fm. The notation and formalism used here is the same as that of Ref. [15].

$n+{}^{93}$Nb
$A_{HF}=48.50$; $\lambda=0.86\times10^{-2}$; $a_{HF}=0.67$; $r_{HF}=1.245$
$A_s=9.6$; $B_s=9.6$; $C_s=0.20\times10^{-3}$; $m=2$; $a_s=0.48$; $r_s=1.28$
$A_v=11.52$; $B_v=75.0$; $n=2$; $E_F=-8.029$; $q=2.0$
$V_{so}=6.0$; $a_{so}=0.60$; $r_{so}=1.08$

II. DISPERSIVE OPTICAL MODEL ANALYSIS FOR ^{93}Nb

The DOM for the $\vec{n}+{}^{93}\vec{\mathrm{N}}$b system used a database that included $\sigma(\theta)$, $A_y(\theta)$, and σ_T up to 80 MeV. The differential cross-section data included that of Ref. [17] from 1.5 to 4.0 MeV, Ref. [18] from 4.5 to 9.0 MeV, Ref. [19] at 11.0 MeV, Ref. [20] at 10.0, 12.0, 14.0, and 17.0 MeV, Ref. [21] at 14.7 MeV, and Ref. [22] at 20.0 MeV. The analyzing power data included two distributions from Ref. [20] at 10.0 and 14.0 MeV. The total cross-section data were from Refs. [17,23] from 0.040 to 20.0 MeV and Ref. [24] from 5.0 to 80 MeV.

The DOM model was built using grid search techniques similar to those described in the companion paper [15] for ^{27}Al and ^{59}Co. The potential parameters for ^{93}Nb are given in Table I, where we use the notation and definitions introduced in Ref. [15]. As can be seen in Fig. 1, this DOM potential provides a good overall description of the measurements available for the elastic scattering cross section $\sigma(\theta)$ and analyzing power $A_y(\theta)$. Figure 2 displays reasonable agreement between the DOM predictions and total cross-section data, and includes similar comparisons for ^{27}Al and ^{59}Co, reproduced from Ref. [15].

III. SPIN-SPIN CROSS-SECTION ANALYSES

Prior to describing the optical model calculations performed for spin-spin cross sections, we draw the reader's attention to the strong correlation existing between the zeros in the spin-spin cross section and the extrema of the total cross section, σ_T, as can be seen by comparing Figs. 2 and 3. This phenomena may qualitatively be explained as a byproduct of the Ramssauer effect governing the E-dependent pattern of σ_T. For a neutron and target that are both transversely polarized, the spin-spin cross section is defined as [7]

$$\sigma_{ss}=\tfrac{1}{2}[\sigma_T(U+U_{10})-\sigma_T(U-U_{10})], \tag{1}$$

where U_{10} stands for the central spin-spin potential and U for the optical model potentials. This definition, which stems from an approximation which neglects the spin-orbit coupling and the tensor spin-spin components, has been shown to be reliable [7] and should not obscure our analyses. Note that this definition of the transverse spin-spin cross section corresponds to $\Delta\sigma_T$ used by the few-nucleon community (the "T" here standing for "transverse"), except for a change of sign [25]. Equation (1) may be formally reexpressed through a Taylor series expansion to first order as

$$\sigma_{ss}(E)\approx U_{10}\left[\frac{dU}{dE}\right]^{-1}\frac{d}{dE}[\sigma_T(E)]. \tag{2}$$

In our optical model study, the leading-order term in the spin-spin potential is the central component [5]

$$U_{10}(r)=F_{10}(r)\hat{I}\cdot\hat{s}. \tag{3}$$

The tensor component of the spin-spin potential is not included since we are only concerned with transverse polarization of the beam and target. If we define $\vec{r}$, $\vec{s}$, and $\vec{I}$ as the neutron-nucleus radial vector, neutron spin, and target spin, respectively, then $r=|\vec{r}|$ and the spin operators appear in the normalized forms $\hat{s}=\vec{s}/|\vec{s}|$ and $\hat{I}=\vec{I}/|\vec{I}|$. The $F_{10}(r)$ contains both surface and volume form factors as well as the corresponding potential strengths,

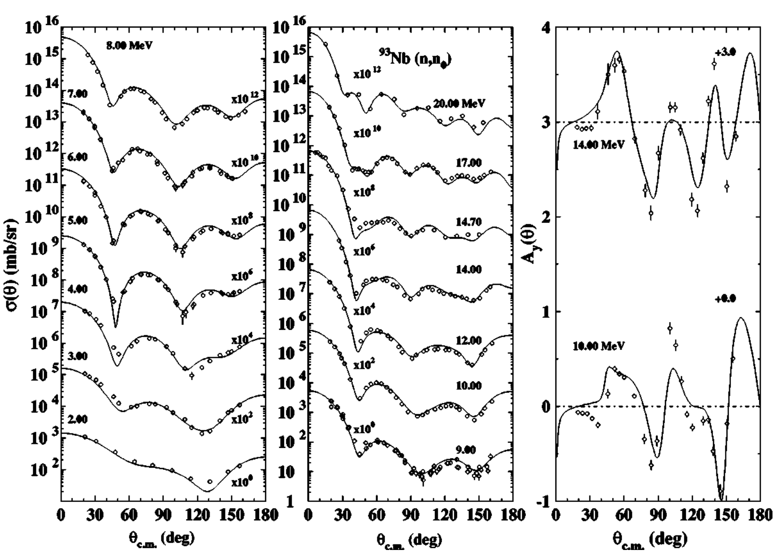

FIG. 1. $\sigma(\theta)$ and $A_y(\theta)$ data for $n+{}^{93}$Nb compared to DOM calculations. The calculations include contributions from compound-elastic scattering at low energies. The large negative excursions of $A_y(\theta)$ at small angles is due to the Mott-Schwinger interaction.

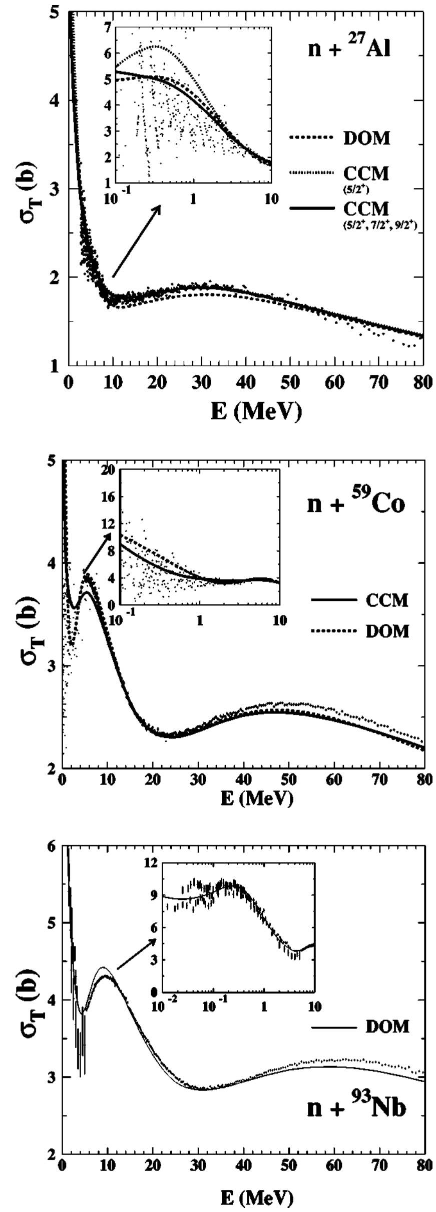

FIG. 2. Total cross-section data compared to the DOM and CCM calculations for ^{59}Co and ^{27}Al and to the DOM calculations for ^{93}Nb.

$$F_{10}(r) = V_{ss}^{(s)} 4a_{ss}\frac{d}{dr}f(r,R_{ss},a_{ss}) + V_{ss}^{(v)} f(r,R_{ss},a_{ss}). \qquad (4)$$

The f is a Woods-Saxon shape in which $R_{ss}=r_{ss}A^{1/3}$ is assumed. For simplicity, $F_{10}(r)$ is taken as a real function.

In the present work, the central spin-spin potential was determined from the energy dependence exhibited in spin-spin cross sections measured over a broad energy range for ^{27}Al [5,6], ^{59}Co [4,26–28], and ^{93}Nb [6,29]. For this purpose, Eqs. (3) and (4) were used to represent the spin-spin interaction, U_{10}. The central and spin-orbit potentials, U, were taken from Ref. [15] for ^{27}Al and ^{59}Co and from the present work for ^{93}Nb. For each nucleus independently, grid searches of the spin-spin potential parameters were done in order to achieve the best possible representations of existing σ_{ss} measurements. All of the analyses were performed with the ECIS code [30] run in the external input mode. The results gave parameter sets that were similar for ^{27}Al, ^{59}Co, and ^{93}Nb using either spherical (DOM) or deformed (CCM) central and spin-orbit potentials.

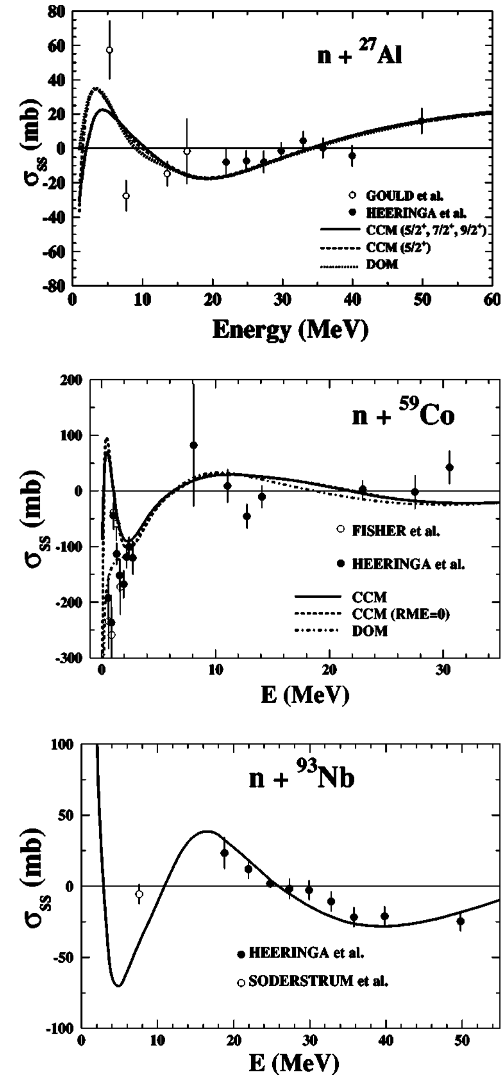

FIG. 3. Spin-spin cross-section data compared to the DOM and CCM calculations for ^{59}Co and ^{27}Al and to the DOM calculations for ^{93}Nb.

Figure 3 displays the σ_{ss} predictions using our DOMs and CCMs. For ^{27}Al, the DOM predictions fit most of the σ_{ss} data above 10 MeV and are close to the measurement at 6 MeV where a maximum occurs. In the vicinity of the 7.5 MeV datum, our predictions fail badly. The nucleus ^{59}Co is one for which many σ_{ss} data are available, especially at energies as low as 1 MeV. For this nucleus, the DOM analysis in the range 100 keV to 3 MeV leads to σ_{ss} predictions which describe the measurements well, except for the spike at $\sim$1.6 MeV, which may signal resonance effects taking place. For ^{93}Nb, the predictions and measurements are in nice agreement above 18 MeV. On the other hand, the datum at 7.5 MeV is far above the predictions. At this energy, we could have included the datum from Ref. [29] for longitudinal geometry, in addition to the one for transverse geometry (since our analysis neglects the tensor spin-spin components). However, because the longitudinal datum is consistent with the transverse datum and has a larger uncertainty, we have not displayed it.

The CCM predictions are shown in Fig. 3 for the deformed nuclei ^{27}Al and ^{59}Co. For ^{27}Al, two sets of calculations are illustrated. The first one is for a coupling basis which includes the first three members of the ground-state rotational band. This three-level calculation (solid line) coincides with the DOM predictions (dotted line) only above 13 MeV, an energy range where the present predictions and the measurements are in agreement. Below 10 MeV, the three-level calculations do not match with the data at 5.5 and 7.5 MeV. A simpler coupled-channel analysis in which only the ground-state level is considered leads to results (dashed curve) that are similar to the other models at energies above 13 MeV. Below 10 MeV, the one-level predictions are close in shape and magnitude to those based on the DOM analyses. None of these three model analyses are able to explain the measurements below 10 MeV, even though our dedicated optical models offer a good overall description of the other scattering and total cross-section reaction measurements. Switching off the reorientation matrix elements in the coupled-channel calculations does not cure this deficiency.

Similar CCM analyses are shown for ^{59}Co. As discussed in Ref. [15], despite the fact that the level scheme of ^{59}Co suggests a vibrational structure, we used a rotational model that coupled the ground state only to itself. Because it overestimates the reorientation effect, this simple model enables us to judge the degree to which a deformed potential alters the spin-spin predictions for ^{59}Co. Good agreement between predictions and measurements are obtained above 3 MeV. Below this energy, the CCM predictions are systematically too high. Turning off the reorientation matrix elements does not improve the fit.

By mildly constraining the grid search method, it was possible to compromise on the spin-spin geometry and potential strength parameters for the three scattering systems. All the results discussed above use $r_{ss}=1.0$ fm and $a_{ss}=0.55$ fm for the radius and diffuseness, respectively. The strengths of the spin-spin potential are $V_{ss}^{(s)}=0.8$ MeV and $V_{ss}^{(v)}=0.2$ MeV in the DOM analyses and $V_{ss}^{(s)}=0.6$ MeV and $V_{ss}^{(v)}=0.4$ MeV in the CCM analyses. The radial shapes for the $F_{10}(r)$ potential of Eq. (4) are displayed in Fig. 4 for the ^{59}Co CCM (solid curve) and DOM (dotted) analyses. These shapes, as well as those for ^{27}Al and ^{93}Nb, are peaked at the nuclear surface, in good agreement with earlier phenomenological determinations [7,8].

The volume integrals J_{ss}/A determined for each nucleus and model analysis are listed in Table II. The J_{ss}/A values deduced from the coupled-channels analyses are about 10% lower than those from the dispersive model analyses. This difference provides an estimate of the uncertainty of our determination of J_{ss}/A for a particular nucleus.

Because we were able to fit the spin-spin cross-section data using the same strength parameters and surface-peaked geometry for all three scattering systems, the J_{ss}/A values of Table II decrease with increasing A. This dependence is not as strong as the $1/A$ dependence suggested by Satchler [31]. However, it is interesting to compare our results to those of Ref. [8] for $\vec{p}+^{13}$C. The "best fit" spherical spin-spin potential of Ref. [8] gives a J_{ss}/A value of 21.5 MeV fm^3, suggesting that the volume integral decreases more abruptly with increasing A in the regime of light nuclei.

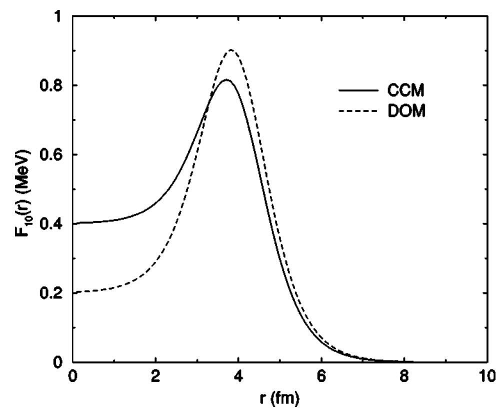

FIG. 4. Radial shapes of the spin-spin potentials for the $\vec{n}+^{59}\vec{\mathrm{Co}}$ system.

The present analysis is based on a reaction model that neglects the spin-orbit coupling and the tensor spin-spin potentials. While the impact of neglecting the spin-orbit coupling appears to be negligible for medium to heavy nuclei [7], tensor interactions must be considered to make our J_{ss}/A values more realistic. We can estimate the effect of ignoring the tensor interactions by considering the results of other studies. The microscopic model of Ref. [7] calculates spin-spin cross sections as superpositions of three components, with the component stemming from the spherical operator predominating. The effect of adding the two other components, due to tensor interactions, is to increase the magnitude of the spin-spin cross-section predictions by about 30%. This suggests that the present study, by leaving out tensor interactions, has overestimated the spherical spin-spin potential and the J_{ss}/A values. This is consistent with the optical model results of Ref. [8], which find that J_{ss}/A goes down by about 30% (from 21.5 to 15.3 MeV fm^3) when a tensor potential is added. From the above considerations, we estimate that adding a tensor term to our models would result in a reduction of the values quoted in Table II by about 30%. Therefore, we give our overall determination of J_{ss}/A as being between 4 and 7 MeV fm^3. These results are consistent with previous empirical determinations [5,6,28] but systematically lower than predictions based on NN effective forces [32–34].

TABLE II. Volume integrals of the spin-spin potentials (see discussion in text).

Target nucleus	DOM J_{ss}/A (MeV fm^3)	CCM J_{ss}/A (MeV fm^3)
^{27}Al	9.30	8.37
^{59}Co	7.06	6.55
^{93}Nb	6.08	

IV. CONCLUSIONS

Several optical model potentials designed to describe neutron scattering and reactions from ^{27}Al, ^{59}Co, and ^{93}Nb have been used in a detailed analysis of spin-spin cross-section measurements. All of these optical model potentials lead to predictions which agree with the available spin-spin data above ~10 MeV. Below this energy, the results of our analyses are ambiguous, partly because they depend heavily on which reaction model is adopted. We caution that one should not rule out the possibility that in this lower energy range, compound processes compete with direct-reaction processes and that the interference of these two confuse the spin-spin issue.

We conclude that the volume integral, J_{ss}/A, of the leading-order term in the spin-spin potential is between 4 and 7 MeV fm^3, and decreases somewhat as A increases. Compared to typical values of the volume integral, J_v/A, of the real central potentials (about 400 MeV fm^3), J_{ss}/A is very weak (between 1% and 2% of J_v/A). Our values for J_{ss}/A are consistent with previous phenomenological analyses and suggest that the volume integrals of the spin-spin terms in the t-matrix and g-matrix analyses of Ref. [33] and Ref. [34], respectively, are too strong. Our present empirical information may be of interest for improving the parametrizations of NN effective forces at low energy.

ACKNOWLEDGMENTS

This work was supported in part by the U.S. Department of Energy, under Grant No. DE-FG02-97ER41033. The authors acknowledge valuable conversations with C.R. Gould.

[1] H. Feshbach, Annu. Rev. Nucl. Sci. **8**, 49 (1958).
[2] J. S. Blair, M. P. Baker, and H. S. Sherif, Phys. Lett. **60B**, 25 (1975).
[3] W. J. Thompson, Phys. Lett. **65B**, 309 (1976).
[4] W. Heeringa and H. Postma, Phys. Rev. C **27**, 2012 (1983).
[5] C. R. Gould, D. G. Haase, L. W. Seagondollar, J. P. Soderstrum, K. E. Nash, M. B. Schneider, and N. R. Roberson, Phys. Rev. Lett. **57**, 2371 (1986).
[6] W. Heeringa, H. O. Klages, Chr. Wolfl, and R. W. Finlay, Phys. Rev. Lett. **63**, 2456 (1989).
[7] T. L. McAbee, W. J. Thompson, and H. Ohnishi, Nucl. Phys. **A509**, 39 (1990).
[8] B. v. Przewoski, P. D. Eversheim, F. Hinterberger, U. Lahr, J. Campbell, J. Gotz, M. Hammans, R. Henneck, G. Masson, I. Sick, and W. Bauhoff, Phys. Rev. Lett. **64**, 368 (1990).
[9] R. Henneck, G. Masson, P. D. Eversheim, R. Gebel, F. Hinterberger, U. Lahr, H. W. Schmitt, J. Schleef, and B. v. Przewoski, Nucl. Phys. **A571**, 541 (1994).
[10] V. M. Hannen *et al.*, Phys. Rev. C **67**, 054321 (2003).
[11] A. H. Hussein and H. S. Sherif, Phys. Rev. C **8**, 518 (1973).
[12] F. D. Becchetti and G. W. Greenlees, Phys. Rev. **182**, 1190 (1969).
[13] R. L. Varner, W. J. Thompson, T. L. McAbee, E. J. Ludwig, and T. B. Clegg, Phys. Lett. B **185**, 6 (1987).
[14] A. J. Koning and J. P. Delaroche, Nucl. Phys. **A713**, 231 (2003).
[15] M. M. Nagadi, C. R. Howell, W. Tornow, G. J. Weisel, M. A. Al-Ohali, R. T. Braun, H. R. Setze, Zemin Chen, R. L. Walter, J. P. Delaroche, and P. Romain, Phys. Rev. C **68**, 044610 (2003).
[16] J. Dechargé and D. Gogny, Phys. Rev. C **21**, 1568 (1980).
[17] A. B. Smith, P. T. Guenther, and J. F. Whalen, Nucl. Phys. **A415**, 1 (1984).
[18] A. B. Smith, P. T. Guenther, and R. D. Lawson, Argonne National Laboratory Report No. ANL-NDM-91, 1981.
[19] J. C. Ferrer, J. D. Carlson, and J. Rapaport, Nucl. Phys. **A275**, 325 (1977).
[20] R. S. Pedroni, R. C. Byrd, G. M. Honoré, C. R. Howell, and R. L. Walter, Phys. Rev. C **43**, 2336 (1991).
[21] C. Jianhua, D. Yunsheng, W. Dairong, L. Xuecai, and W. Siming, EXFOR 32521003 (1988).
[22] R. W. Finlay, W. Walter, A. Marcinkowski, and J. Rapaport, EXFOR 13532002 (1991).
[23] W. P. Poenitz and J. F. Whalen, Argonne National Laboratory Report No. ANL-NDM-80, 1983.
[24] R. W. Finlay, W. P. Abfalterer, G. Fink, E. Montei, T. Adami, P. W. Lisowski, G. L. Morgan, and R. C. Haight, Phys. Rev. C **47**, 237 (1993).
[25] W. S. Wilburn, C. R. Gould, D. G. Haase, P. R. Huffman, C. D. Keith, N. R. Roberson, and W. Tornow, Phys. Rev. C **52**, 2351 (1995).
[26] T. R. Fisher, H. A. Greuch, D. C. Healey, J. McCarthy, D. Parks, and R. Whitmer, Nucl. Phys. **A179**, 241 (1972).
[27] W. Heeringa and H. Postma, Phys. Lett. **61B**, 350 (1976).
[28] W. Heeringa, H. Postma, H. Dobiasch, R. Fischer, H. O. Klages, R. Maschuw, and B. Zeitnitz, Phys. Rev. C **16**, 1389 (1977).
[29] J. P. Soderstrum, C. R. Gould, D. G. Haase, N. R. Roberson, M. B. Schneider, and L. W. Seagondollar, Phys. Rev. C **45**, 326 (1992).
[30] J. Raynal, in *Applied Nuclear Theory and Nuclear Model Calculations for Nuclear Technology Applications*, edited by M. K. Mehta and J. J. Schmidt (World Scientific, Singapore, 1989), p. 506.
[31] G. R. Satchler, Part. Nuclei **1**, 397 (1971).
[32] S. M. Austin, in *The (p,n) Reaction and Nucleon-Nucleon Force*, edited by C. D. Goodman *et al.* (Plenum, New York, 1980), p. 203.
[33] F. Petrovich and W. G. Love, Nucl. Phys. **A354**, 499c (1981).
[34] K. Nakayama and W. G. Love, Phys. Rev. C **38**, 51 (1988).